

FIRST ELECTRON BEAM OF THE THOMX PROJECT*

C. Bruni[†], M. Alkadi, J. N. Cayla, I. Chaikovska, S. Chancé, V. Chaumat, O. Dalifard, N. Delerue, K. Dupraz, M. El Khaldi, N. ElKamchi, E. Ergenlik, P. Gauron, A. Gonnin, E. Goutierre, H. Guler, M. Jacquet, V. Kubytskyi, P. Lepercq, F. Letellier-Cohen, J. C. Marrucho, B. Mercier, E. Mistretta, H. Monard, A. Moutardier, M. Omeich, V. Soskov, F. Wicek
Université Paris-Saclay, CNRS/IN2P3, IJCLab, 91405, Orsay, France,
on behalf of the ThomX collaboration [1].

Abstract

The ThomX accelerator beam commissioning phase is now ongoing. The 50 MeV electron accelerator complex consists of a 50 MeV linear accelerator and a pulsed mode ring. It is dedicated to the production of X-rays by Compton backscattering. The performance of the beam at the interaction point is demanding in terms of emittance, charge, energy spread and transverse size. The choice of an undamped ring in pulsed mode also stresses the performance of the beam from the linear accelerator. Thus, commissioning includes a beam based alignment and a simulation/experimental matching procedure to reach the X-ray beam requirements. We will present the first 50 MeV electron beam obtained with ThomX and its characteristics.

THOMX ACCELERATOR DESCRIPTION

ThomX [2–4] is a compact Compton scattering source hosted in the Paris-Saclay scientific university campus (Orsay, France). The goal is to demonstrate the production of hard X-rays (45 keV) with a flux of 10^{11} - 10^{13} ph/s. The ThomX accelerator complex is composed of a linear accelerator combined with a 50 MeV electron ring. The ThomX linear accelerator is composed of two main warm RF components: the RF gun and the accelerating section that boosts the electrons to the final energy for the ring injection. ThomX RF gun has mainly the same design as the CTF3 model [5, 6] with a nominal RF field amplitude to be reached of 80 MV/m. The accelerating section is lent by Synchrotron SOLEIL. To achieve a final energy of 50 MeV, the energy gain in the section must be 45 MeV [7].

The compactness of the ring allows a high repetition rate of the electron bunch at the Compton interaction point to maximize the X-ray flux. Due to the short Touschek lifetime at this low energy, the ring does not operated in a damped mode, but in a pulsed mode [8]. In such a case, a single electron bunch is injected in the ring every 20 ms. Then, Radiation damping is negligible during the storage time as it is in the order of 1 second. The 20 ms cycle has been chosen to prevent the electron beam degradation due to the Compton collisions that produce the x-rays, and collective effects as Intrabeam scattering [9].

* Work supported by the French "Agence Nationale de la Recherche" as part of the program "investing in the future" under reference ANR-10-EQPX-51 and by grants from Région Ile-de-France

[†] christelle.bruni@ijclab.in2p3.fr

Since the quality of the X-ray production is mostly determined by the electron beam characteristics [10–12], the lack of radiation damping in the ring makes a high quality electron beam essential at the exit of the linac. In fact, the emittance at the interaction point will be dominated by the one achieved by the linac and the transfer line. So the characteristic of the beam coming from the linac should avoid emittance degradation in the transfer line due to collective and chromatic effects. The electron beam properties at the exit of the transfer line strongly dominate the subsequent particle dynamics in the ring and the ultimate machine performances at the interaction point. So, a dedicated tuning of the linac is necessary.

During May 2021, Phase I authorization from the French Nuclear Safety Authority was given. It implies that the beam parameters be limited to 100 pC, 50 MeV, and 10 Hz of repetition rate of the RF source and a limitation on the linac straight section with the impossibilities to send the electron beam into the transfer line and then the ring. The paper first presents the conditioning stage of the linac RF cavities, then the first beam established in 3 days at 37 MeV, and finally the characterisation and optimisation stages that are currently underway.

FIRST ELECTRON BEAM

Different working points have been prepared for 100 pC, 500 pC, and 1 nC. The beam parameters are summarized in Table 1. The first commissioning phase allowed us to accelerate up to 100 pC maximal charge with an expected emittance value of 2π mm mrad according to a rms spot size of 0.3 mm.

Table 1: Summary of the Linac Performances

Charge (nC)	1	0.5	0.1
rms Laser transverse size (mm)	0.5	0.4	0.3
Energy spread at linac output (%)	0.25	0.25	0.25
Normalised Emittance linac output (π mm mrad)	4.4	3	1.5

Following authorization from the French Nuclear Safety Authority (ASN) for the first phase (100 pC, 50 MeV at 10 Hz), the RF conditioning of the ThomX linac was carried out from July to October 2021 in several phases. RF cavities should be conditioned by applying progressive RF power to the system. Up to 9 MW RF power at 10 Hz, LIL section was conditioned in two days in June 2021 as it was in use

before. Whereas the RF gun was first conditioned at 1 Hz and 5 MW in three weeks in September 2021. An other week was needed to reach 6 MW at 10 Hz on October. This dissociation enables us to successively commission all the beam equipment.

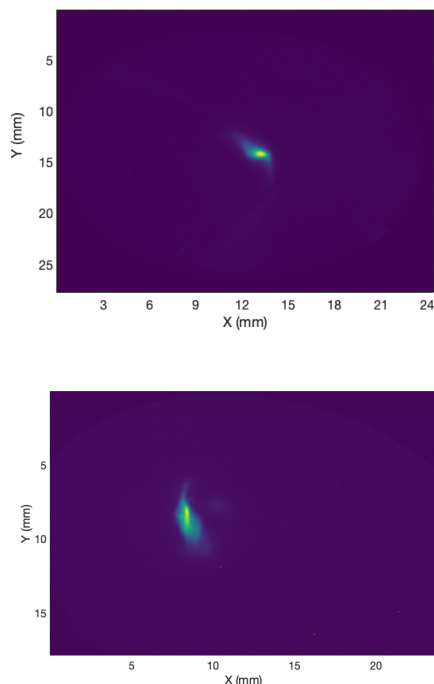


Figure 1: Image retrieved from the YAG:Ce screen light emission from the electron beam at the exit of the RF gun (Top) and at the linac exit (Bottom) the 6th of October 2021.

The 4th of October, the linac commissioning team imaged the first beam from the gun on a YAG screen located 1.2 m from the photocathode [13], as shown in Fig. 1. While waiting for the commissioning of the ICT, the maximum energy phase was adjusted thanks to the knowledge of the behavior of the beam at the exit of the gun (transverse dimension, charge). In this context, we adjusted the RF phase to optimize the energy at the gun's exit. Two solenoids that surround the RF gun are used as a standard emittance compensation scheme. In addition, the solenoids are able to "match" the beam emittance into the first accelerating cavity [14, 15]. The 5th of October, a day of conditioning of the gun was required with the concomitant operation of the solenoids current that we gradually increased. The 6th of October, the focused beam at the entrance of the section was transmitted to the end of the linac. The Fig. 2 shows the raw ICT signals at the gun exit and at the section entrance with 90% transmission. The presence of dark current is clearly indicated with the non zero background level. On October 7, energy measurements were made employing the steerers in the absence of a dipole. Results at the gun exit are shown in [13].

Once the gun was conditioned, the electron beam at the linac exit was obtained within three days. Since then, the

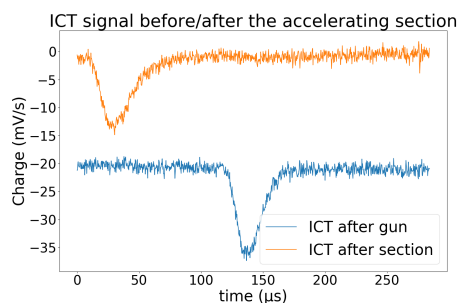


Figure 2: Raw ICT signal versus time at the gun exit (blue) and at the linac exit (red) taken the 6th of October 2021.

use of the equipment, the human machine interface and the measurement scripts have been improved. The beam quality and performances were also improved.

BEAM CHARACTERISATION

At the output of the gun, several diagnostics are available to characterize the beam, an ICT for charge measurement, a screen station for dimensional measurement, and a BPM stripline. The most important parameter to control is the phase between the RF gun and the laser impinging onto the photocathode. A measure of the beam charge as a function of the gun RF phase is shown in Fig. 3. The phase extension of about 100 degrees is obtained very quickly. We recover the typical shape given by the Schottky effect. Indeed, the charge increases according to the voltage at the cathode. The phase giving the maximum charge is shifted by about 40 degrees (value depending on the accelerator gradient) compared to the phase that gives the maximum energy. This is because the electrons are emitted at rest energy, and slide relative to the accelerating wave. Thus the phase giving the maximum energy gain does not coincide with the phase giving the maximum field at the cathode [16]. The gun output energy was also qualified using the relationship between the deviation given by the corrections and the beam energy. The results are shown in Fig. 3 and are in agreement with the measurements of the RF signal amplitude.

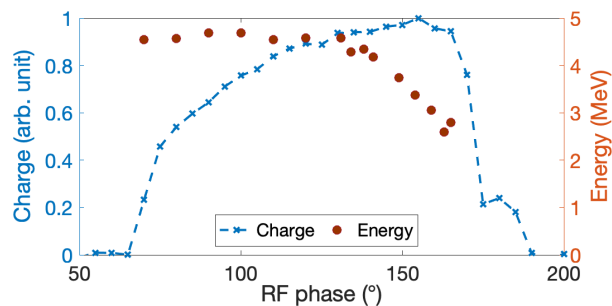


Figure 3: Charge and kinetic energy measured at the exit of the RF gun versus its RF phase the 30th of May 2022. The energy measurements were provided by a steerer and a screen spaced by 0.77 m.

Content from this work may be used under the terms of the CC BY 4.0 licence (© 2022). Any distribution of this work must maintain attribution to the author(s), title of the work, publisher, and DOI

Finally, around the phase of maximum charge, corresponding to the RF focusing maximum, the beam barycentre moves linearly with the RF phase in the case of a laser misalignment. The slope increases with misalignment, and the two axes are unrelated. A measurement of the beam barycenter as a function of phase allows the laser alignment to be corrected using a driven mirror. Figure 4 shows a case of optimization of the alignment of the laser that is converging to a beam on the electromagnetic axis of the RF gun.

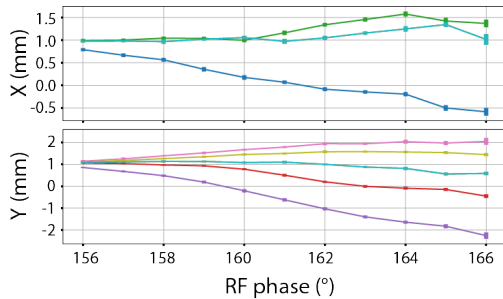


Figure 4: Barycenter of the electron beam versus the RF phase of the gun for different position of the laser on the cathode. The beam position is measured with a BPM located at 0.6 m from the cathode. X indicated the horizontal direction while Y the vertical one.

The behavior of the beam barycentre is monitored as a function of the RF phase 0.6 m downstream the cathode with a BPM for phase values around the one giving the maximum charge. The slope is progressively reduced by adjusting the remote control mirror of the laser. The turquoise curve corresponds to the optimized case. The barycentre of the beam aligned on the electromagnetic axis is here off axis with respect to the zero reference of the BPM, highlighting an alignment problem on the machine head. Magnetic components of a few gauss were identified. Mechanical interventions were carried out to reduce these components.

The focusing solenoid at the exit of the gun is equipped with a translation and rotation stage so that it can be aligned with the electromagnetic axis of the gun. Two methods are used: a classical least-squares optimisation by matrix transport, and an optimisation method based on a correction function. The alignment allows the focusing at the entrance of the accelerator section to be optimised while looking at the beam at the exit of the section 9 m downstream the cathode.

The use of two steerers upstream of the accelerator section is required to ensure 100% beam transmission. Indeed, the diameter of the cells is 19 mm, allowing very limited freedom for the beam trajectory along the 4.5 m of acceleration. The beam can currently be transmitted with and without an RF field in the cavities. We thus obtain a 5 MeV beam at 9 m from the cathode viewed on the screen station using the solenoids as the only focusing element. With an RF field in the section, the phase shifter on the RF guide side of the section is used to adjust the relative phase between the beam at the section entrance and the RF field in the section. A

phase-dependent energy measurement was performed using the steerer after the accelerator section combined with the screen at the end of the linac. The 50 MeV was obtained on the 26th of October. Three weeks were devoted to increase the performance in terms of load, alignment, accelerator gradient of the gun, as well as the repetition rate. The rise to nominal performance (100 pC, 50 MeV, 10 Hz) was a priority in order to initiate the ASN administrative procedure as soon as possible to obtain the phase II authorization, which will allow us to inject into the storage ring and to use a spectrometer as an additional diagnostic to optimise the linac parameters.

To end this paper, a three gradient measurement of the emittance at the linac is presented in Fig. 5. A normalised emittance of 4π mm mrad was measured, corresponding to twice the nominal value to be reached at 100 pC. The order of magnitude obtained is therefore comforting for the further optimisation of the linac for injection into the ring.

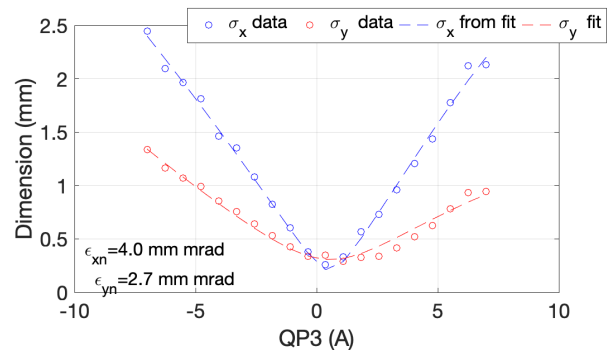


Figure 5: Rms transverse dimension measured on the 6th of April 2022 on the YAG screen located 9 m from the photocathode as a function of the last quadrupole current of a series of three quadrupoles. The emittance is obtained using least mean square methods with transport matrices from the accelerator toolbox of Matlab Middle Layer [9]. ϵ_{xn} is the rms transverse horizontal normalised emittance measured and ϵ_{yn} is the vertical one.

CONCLUSION

The first ThomX linac electron beam has been produced on October 4, 2021. Nominal parameter of charge, energy, repetition rate were achieved three weeks after on the 26th of October. Even optimization are still needed to reach all the nominal parameters as emittance, the beam is ready to be sent in the transfer line [17]. First X-rays are foreseen during the year 2023 depending on the national safety authorization deliveries.

ACKNOWLEDGMENTS

The authors acknowledge all the ThomX collaborators for the long term effort to define and build the accelerator and all the technical staff involved from LAL laboratory from 2007 to 2020 and IJClab since 2020 until now.

REFERENCES

- [1] ThomX collaboration, <https://thomx.ijclab.in2p3.fr/collaboration-thomx/>, [Online; accessed 19-May-2022].
- [2] A. Variola, A. Loulergue, and F. Zomer, “ThomX - Conceptual Design Report,” Tech. Rep., 2009, pp. 1–136, <http://hal.in2p3.fr/in2p3-00448278>
- [3] A. Variola, J. Haissinski, A. Loulergue, and F. Zomer, “ThomX Technical Design Report,” Tech. Rep., 2014, 164 p. <http://hal.in2p3.fr/in2p3-00971281>
- [4] K. Dupraz *et al.*, “The thomx ics source,” *Physics Open*, vol. 5, p. 100051, 2020, doi:<https://doi.org/10.1016/j.physo.2020.100051>
- [5] J. Brossard, M. Desmons, B. M. Mercier, C. P. Prevost, and R. Roux, “Construction of the Probe Beam Photo-injector of CTF3,” in *Proc. EPAC’06*, Edinburgh, UK, Jun. 2006, pp. 828–830.
- [6] W. Farabolini *et al.*, “CTF3 Probe Beam LINAC Commissioning and Operations,” in *Proc. LINAC’10*, Tsukuba, Japan, Sep. 2010, pp. 46–48, <https://jacow.org/LINAC2010/papers/MOP001.pdf>
- [7] M. Alkadi, C. Bruni, M. E. Khaldi, M. Jacquet, and H. Monard, “Electromagnetic and Beam Dynamics Studies of the ThomX LINAC,” in *Proc. IPAC’21*, Campinas, Brazil, May 2021, pp. 2721–2724, doi:10.18429/JACoW-IPAC2021-WEPAB054
- [8] Z. Huang and R. D. Ruth, “Laser-electron storage ring,” *Phys. Rev. Lett.*, vol. 80, pp. 976–979, 5 1998, doi:10.1103/PhysRevLett.80.976
- [9] C. Bruni, J. Haissinski, A. Loulergue, and R. Nagaoka, “Electron Beam Dynamics in the 50 MeV ThomX Compact Storage Ring,” in *Proc. IPAC’11*, San Sebastian, Spain, Sep. 2011, pp. 715–717, <https://jacow.org/IPAC2011/papers/MOPS050.pdf>
- [10] M. Jacquet and C. Bruni, “Analytic expressions for the angular and the spectral fluxes at Compton X-ray sources,” *Journal of Synchrotron Radiation*, vol. 24, no. 1, pp. 312–322, 2017, doi:10.1107/S1600577516017227
- [11] K. Deitrick *et al.*, “Intense monochromatic photons above 100 keV from an inverse Compton source,” *Phys. Rev. Accel. Beams*, vol. 24, p. 050701, 5 2021, doi:10.1103/PhysRevAccelBeams.24.050701
- [12] T. Akagi *et al.*, “Narrow-band photon beam via laser Compton scattering in an energy recovery linac,” *Phys. Rev. Accel. Beams*, vol. 19, p. 114701, 11 2016, doi:10.1103/PhysRevAccelBeams.19.114701
- [13] A. Moutardier *et al.*, “Characterization of the Electron Beam Visualization Stations of the ThomX Accelerator,” Bangkok, Thailand, Jun. 2022, presented at IPAC’22, Bangkok, Thailand, Jun. 2022, paper MOPOPT006, unpublished.
- [14] L. Serafini and J. B. Rosenzweig, “Envelope analysis of intense relativistic quasilaminar beams in rf photoinjectors: A theory of emittance compensation,” *Physical Review E*, vol. 55, no. 6, pp. 7565–7590, 1997, doi:10.1103/PhysRevE.55.7565
- [15] L. Garolfi, C. Bruni, M. E. Khaldi, and C. Vallerand, “Beam Dynamics for the ThomX Linac,” in *Proc. IPAC’17*, Copenhagen, Denmark, May 2017, pp. 4121–4123, doi:10.18429/JACoW-IPAC2017-THPIK008
- [16] T. Vinatier, C. Bruni, and P. Puzo, “Analytical modeling of longitudinal beam dynamics in an RF-gun: From almost zero to relativistic velocities,” *Nuclear Instruments and Methods in Physics Research A*, vol. 953, paper 162914, p. 162914, 2020, doi:10.1016/j.nima.2019.162914
- [17] I. Chaikovska, C. Bruni, S. Chancé, A. R. Gamelin, H. Monard, and A. Loulergue, “Status of the Preparation to the Commissioning of the ThomX Storage Ring,” in *Proc. IPAC’16*, Busan, Korea, May 2016, pp. 833–836, doi:10.18429/JACoW-IPAC2016-MOPOW052